Control of Laminar Separation Over Airfoils by Acoustic Excitation

K. B. M. Q. Zaman* and D. J. McKinzie*
NASA Lewis Research Center, Cleveland, Ohio 44135

The effect of acoustic excitation in reducing "laminar separation" over two-dimensional airfoils at low angles of attack is investigated experimentally. The separation involves a laminar unattached flow on the suction side, which is reattached effectively by even a small-amplitude excitation when the frequency is appropriate. Airfoils of two different cross sections, each with two different chord lengths, are studied in the chord Reynolds number range of 25,000 $< R_c <$ 100,000. While the amplitude of the excitation-induced velocity perturbation is kept constant at a reference point within the flowfield, it is found that the most effective excitation frequency scales as $U_\infty^{3/2}$. The parameter $St/R_c^{1/2}$ corresponding to the most effective frequency for all of the cases studied falls in the range of 0.02 to 0.03, with St being the Strouhal number based on the chord.

Nomenclature

c	= airfoil chord
C_l	= lift coefficient
f_p	= excitation frequency
f_{mn}	= tunnel cross-resonance frequency with m sound pressure nodes in y and n sound pressure nodes in z
L_r	= sound pressure level at reference microphone location
R_c	= chord Reynolds number
St	= Strouhal number, $f_p c/U_\infty$
U, V	= mean velocities in x and y directions, respectively
$\langle U \rangle$	= mean velocity measured with a single hot wire approximating $(U^2 + V^2)^{1/2}$
U_∞	= freestream U
u', v', w'	= rms velocity fluctuations in x, y, z directions; subscript r denotes values at reference location
$\langle u' \rangle, \langle u'_f \rangle$	= rms total and fundamental fluctuation in the direction of $\langle U \rangle$, as measured by a single hot wire
$\langle u' \rangle(f)$	= one-dimensional spectrum of $\langle u' \rangle$
$\langle u'_r \rangle$	= $(u'^2_r + v'^2_r)^{1/2}$
x, y, z	= streamwise, transverse, and spanwise coordinates
x'	= streamwise distance from leading edge
α	= angle of attack
θ	= momentum thickness, subscript s denotes value at separation point

Introduction

SEVERAL experiments have demonstrated that artificial excitation can reduce the tendency toward separation in the flow over an airfoil and thereby improve its performance.[1-8] The separation process and the effect of excitation on it have been noted to be different depending on the ranges of the angle of attack and the Reynolds number.[5] Although at all R_c the flow separates ultimately at large α (post-stall), an unsteady separation may occur around the static stall condition.[5,9] At sufficiently low R_c, on the other hand, extensive separation on the suction side may take place even at low α. As this condition is approached with decreasing R_c for a fixed α, the laminar boundary layer fails to overcome the adverse pressure gradient and separates and forms an unattached free shear layer or a "long bubble" on the upper surface.[10,11] This

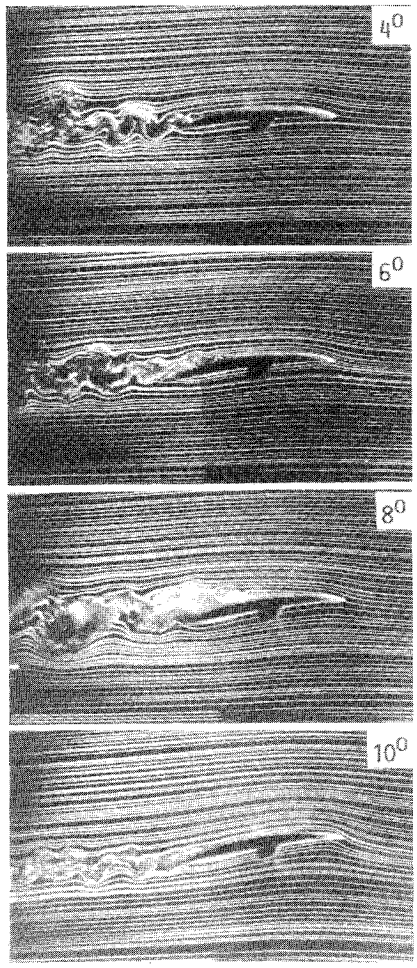

Fig. 1 Smoke-wire flow visualization pictures for various α for LRN airfoil (c = 10.2 cm) at $R_c = 4 \times 10^4$ (Ref. 5).

Presented as Paper 89-0565 at the AIAA 27th Aerospace Sciences Meeting, Jan. 9-12, 1989, Reno, NV; received Nov. 6, 1989; revision received April 18, 1990; accepted July 5, 1990.

*Aerospace Engineer, Internal Fluid Mechanics Division, Mail Stop 5-11. Member AIAA.

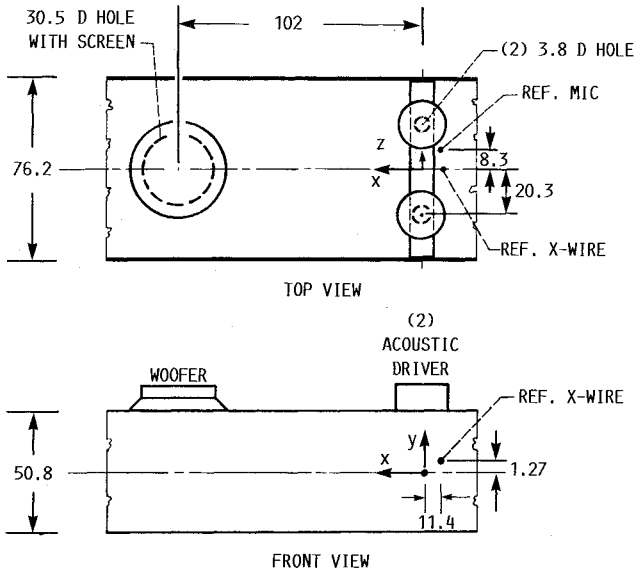

Fig. 2 Schematic of wind-tunnel test section. Dimensions are in centimeters.

process is accompanied by a rapid deterioration of the airfoil performance, approximately in the range $R_c < 100{,}000$ for the airfoils investigated in the present study.

The low-α separation at $R_c = 40{,}000$ is illustrated in Fig. 1 by visualization pictures taken from Ref. 5. Note that the flow on the suction side is separated for all of the lower α but has reattached at the highest α, presumably due to earlier transition of the separated shear layer in that condition. Stability analysis[5] indicated that the boundary layer prior to separation for the low-α cases must be stable and thus laminar. The present data, as discussed later, also satisfy laminar boundary-layer separation criterion.[10] Thus, the flow separation at the low α and low R_c is simply referred to in the following as "laminar separation." Note that laminar boundary-layer separation can also occur prior to the formation of a "short bubble"[11] as well as in post-stall conditions. But here we consider only the laminar separation, with the effect of acoustic excitation being the focus of the study.

In the references cited earlier, the effect of artificial excitation has been studied primarily for post-stall conditions. References 2, 3, and 5 provided some data showing that acoustic excitation can also reduce the extent of the laminar separation. However, the excitation data in all previous studies covered only limited parametric ranges and are insufficient to address the scaling of the effective excitation parameters in any of the situations described earlier.

Recently, Nishioka et al.[12] carried out an acoustic excitation experiment and stability analysis for the flow over a flat-plate model having a sharp leading edge. A main conclusion was that the excitation primarily acted on the inviscid instability of the separated shear layer to produce the observed effects. However, it is not clear that this could be applicable to other situations, e.g., to boundary layers separating from a smooth surface[13] as in the case of an airfoil having a rounded leading edge. The complex nature of the problem at hand must be borne in mind. The excitation has to act on the separated flow, yet the purpose is to achieve, and maintain, reattachment or a tendency thereof. Under the excitation, the mean flow and the corresponding stability characteristics may be quite different. For example, in the ideal case of complete reattachment, there no longer would be a separated shear layer, and the excitation perhaps would have to act on the viscous boundary-layer instability to maintain the reattachment. Therefore, the parameters for optimum excitation, should pertain primarily to the stability of the excited flowfield, even though the corresponding unexcited flowfield has to be influenced sufficiently. At this stage, clearly a lot more experimentation as well as analysis are called for to shed further light into the mechanisms. The present experiment is a step in that direction.

The goal in the experiment was to determine the envelopes of excitation frequencies effectively reducing the laminar separation. The experiment was designed to cover a wide f_p range, and the available parametric ranges were explored systematically. The tunnel resonant frequencies, as will be addressed further, were given due consideration. The effect on the lift coefficient has been used as the primary diagnostic for assessing the influence of the excitation. The assumption that two dimensionality in the flowfield prevails is implicit in the study, and all flow measurements are reported for one span location. The scaling of the effective frequency envelopes is then analyzed. The flowfield details for a specific excitation case are compared with the corresponding unexcited case and discussed in light of boundary-layer separation criteria and stability analyses.

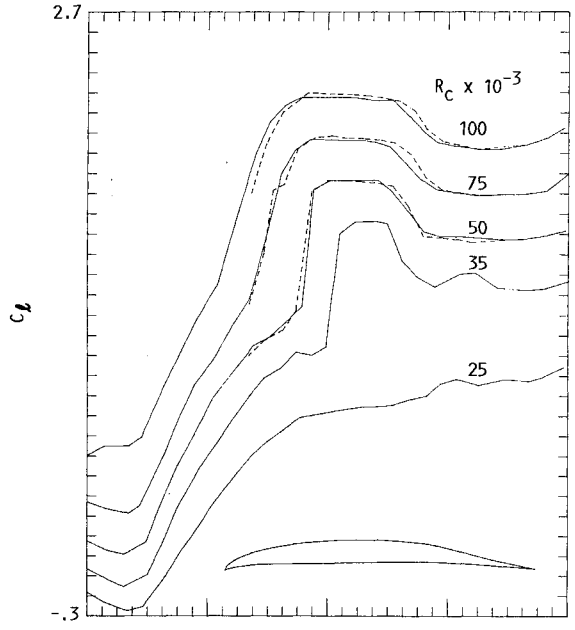

Fig. 3a C_l vs α for $c = 12.7$ cm LRN airfoil at various R_c. Ordinate applies to bottom curve; others are staggered successively by one division. Solid curves, increasing α; dashed curves, decreasing α.

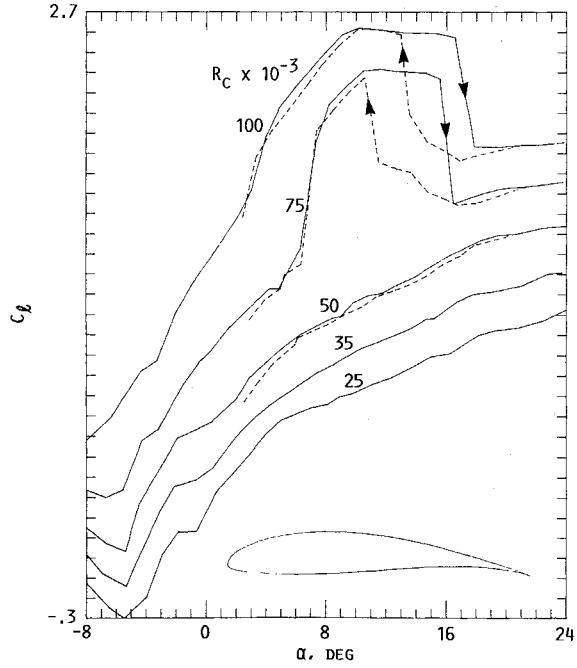

Fig. 3b C_l vs α for $c = 12.7$ cm Wortmann airfoil.

Experimental Facility

The experiments were carried out in the NASA Lewis low-speed wind tunnel, which has been described in detail elsewhere.[9] A schematic of the test section is shown in Fig. 2. The freestream turbulence intensity is less than 0.1%. Two-dimensional models of an LRN-(1)-1007 and a Wortmann FX 63-137 airfoil were used.[9] For each type, two models with chords of 12.7 and 25.4 cm were employed. The airfoils were supported at midchord and spanned the entire test section. Two acoustic drivers (Altec Lansing 291-16K, rated 0.5–20 kHz) and a 40.6-cm woofer (Altec Lansing 515-8G, rated 40 Hz to 4 kHz) were mounted on the ceiling. Even though the amplitude fell off, the woofer could be used for excitation at f_p as low as 15 Hz. The sound from the woofer entered the test section through a 30.5-cm-diam opening. The opening was covered with a 64-mesh screen. The sound from the acoustic drivers entered the test section via 3.5-cm holes in the ceiling. For all data presented only one speaker was used at a time; for $f_p < 700$ Hz the woofer was used, and for $f_p > 700$ Hz one of the acoustic drivers was used.

A ¼-in. (B & K) microphone, flush-mounted on the ceiling, was used to measure a reference sound pressure level (L_r). A crossed hot-film probe (DISA 55R53) was used to measure velocity fluctuation amplitudes (u' and v') at a reference location about 0.4 C upstream of the airfoil leading edge (Fig. 2). The DISA 55R53 probe was replaced by a DISA 55R54 probe to measure w'. A computer-controlled traversing mechanism was used to move a single hot wire to measure the velocity field around the airfoil. The coordinate origin is at the tunnel midheight ($y = 0$) and midspan ($z = 0$) and at the airfoil midchord ($x = 0$). For convenience the streamwise coordinate (x') for some data has been referenced to the airfoil leading edge. Lift and drag were measured by a balance mechanism as described in Ref. 9. For the purposes of this paper, only C_l data are presented. Let us note, however, that an increase in the lift under acoustic excitation was in almost all cases accompanied by a corresponding decrease in the drag. The repeatability in C_l, which was poor at low R_c primarily due to the resolution of the load cell, was within ±0.05 for the worst case at the lowest R_c.

Results and Discussion

Airfoil Characteristics Without Excitation

C_l vs α for the $c = 12.7$ cm LRN airfoil is shown in Fig. 3a for various R_c. The cross section of the airfoil is shown by the inset in the figure. For $R_c \geq 35{,}000$, the C_l curves are marked by a "sag" at low α (Ref. 2). This is due to the laminar separation. At relatively higher α, the airfoil recovers to the high lift condition due to reattachment of the flow occurring naturally (Fig. 1). This occurs presumably due to a steeper adverse pressure gradient causing an earlier transition of the separated shear layer at the higher α; thus, a "short" separation bubble is expected near the leading edge which is not adequately resolved for the $\alpha = 10$ deg case in Fig. 1. The sag in the C_l curve (Fig. 3a) becomes more pronounced at lower R_c. At $R_c = 25{,}000$, the flow remains separated throughout the α range, and the airfoil has completely lost its efficiency in producing high lift.

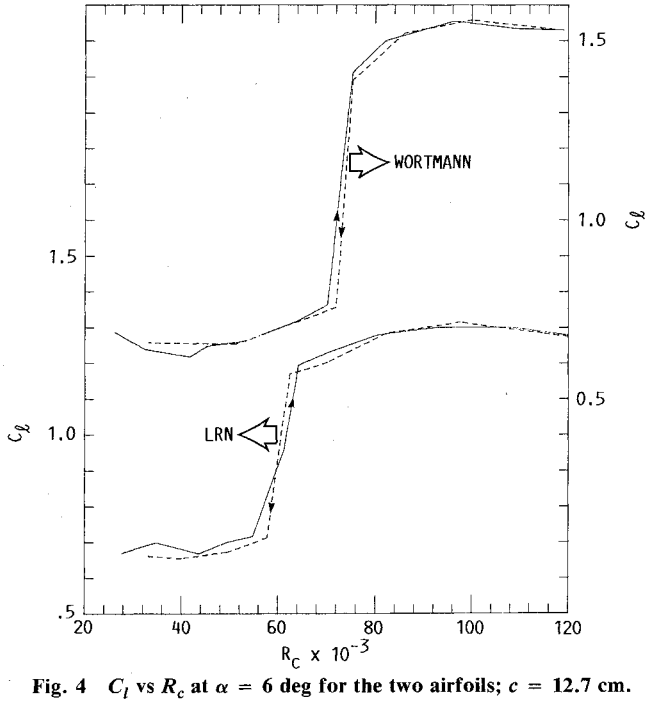

Fig. 4 C_l vs R_c at $\alpha = 6$ deg for the two airfoils; $c = 12.7$ cm.

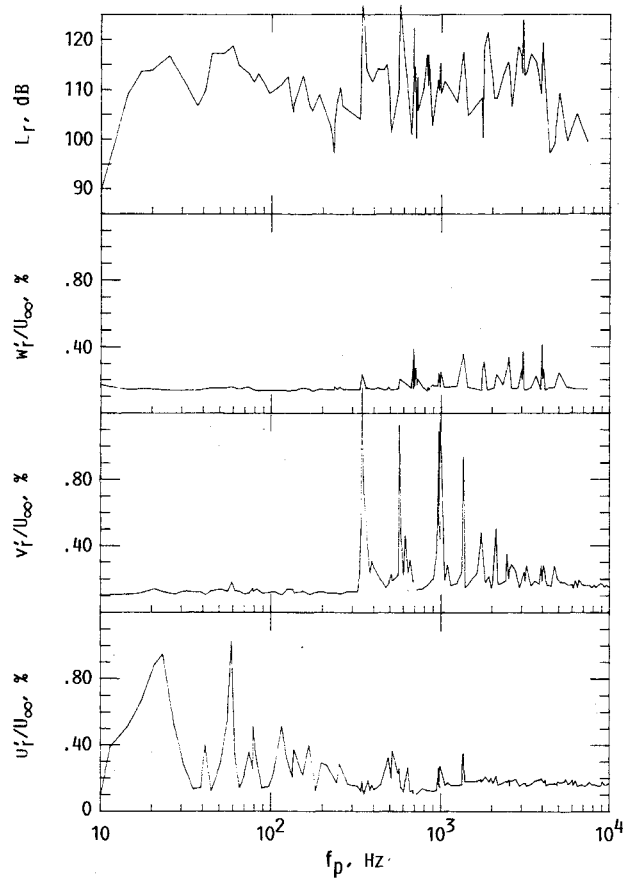

Fig. 5 Reference amplitude parameters vs f_p. Hot wire at $x = -11.4$ cm, $y = 1.27$ cm, and $z = 0$; microphone located as shown in Fig. 2. $c = 12.7$ cm LRN airfoil at $\alpha = 6$ deg with $R_c = 50{,}000$.

Essentially the same behavior is observed with the Wortmann airfoil (Fig. 3b). Complete separation at all α commences around $R_c = 50{,}000$ in this case. Another difference is in the stall characteristics. The Wortmann airfoil clearly shows stall hysteresis, whereas the LRN airfoil does not. The former is of the leading-edge stall type, whereas the latter is approximately of the trailing-edge stall type.[9] In the following attention is focused on the laminar separation at low α; unless otherwise stated, all subsequent data are for $\alpha = 6$ deg.

The Reynolds number effect on the C_l of the two airfoils is shown in Fig. 4. Clearly, the laminar separation at $\alpha = 6$ deg persists up to $R_c \approx 60{,}000$ for the LRN airfoil and up to $R_c \approx 75{,}000$ for the Wortmann airfoil. Although these data are for the $c = 12.7$ cm models, the jump to the higher C_l occurred at somewhat higher R_c with the $c = 25.4$ cm models (data not shown). Note that the jump in the C_l, associated with the elimination of the laminar separation, does not involve hysteresis even for the Wortmann airfoil.

Tunnel Resonance

The tunnel resonance characteristics were documented by measuring the reference velocity and sound pressure ampli-

tudes while exciting the flow with the loudspeakers. The LRN airfoil at $\alpha = 6$ deg was in the flow with $R_c = 50{,}000$. As indicated earlier, the woofer was used for $f_p < 700$ Hz and one acoustic driver for $f_p > 700$ Hz. The reference velocity amplitudes and L_r were measured while f_p was varied in discrete steps. The input voltage to each speaker was held constant. The voltage to the woofer was chosen arbitrarily, but the voltage to the acoustic driver was chosen so that L_r was the same at 700 Hz when excited by either speaker. These data are shown in Fig. 5.

The u'_r data indicate that longitudinal resonances are set up at the lower end of the f_p range covered. The 23-Hz peak corresponds to the half-wave resonance involving the entire length of the tunnel. The 59-Hz peak is the half-wave resonance corresponding to the length of the test section, on either end of which the cross-sectional area diverges. Resonances at several harmonics of 59 Hz are also apparent. Note

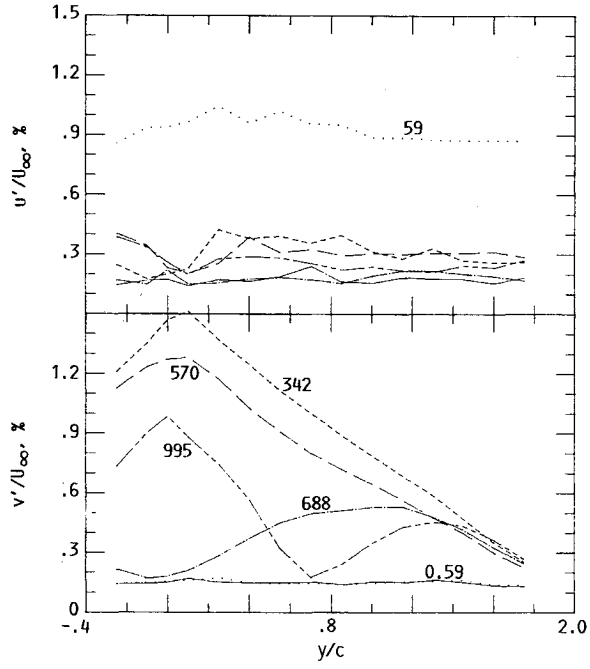

Fig. 6a The u' and v' amplitudes vs y measured at $x = -11.4$ cm and $z = 0$ for indicated f_p values. Same flow as that in Fig. 5.

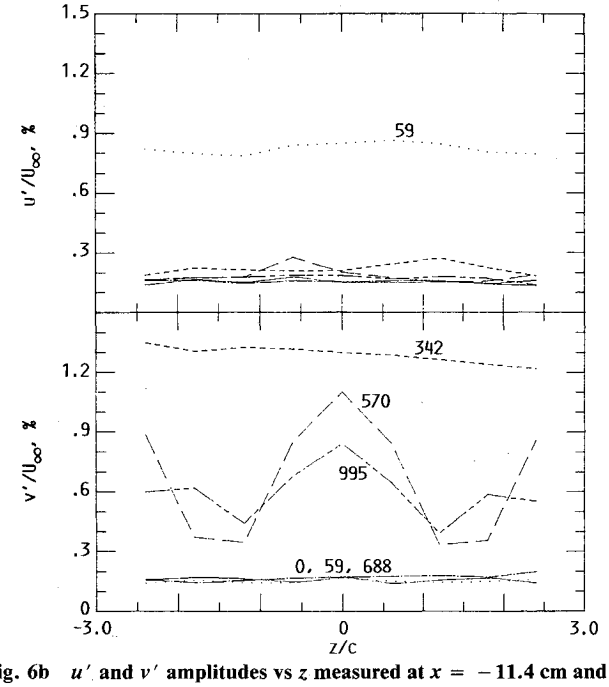

Fig. 6b u' and v' amplitudes vs z measured at $x = -11.4$ cm and $y = 1.27$ cm.

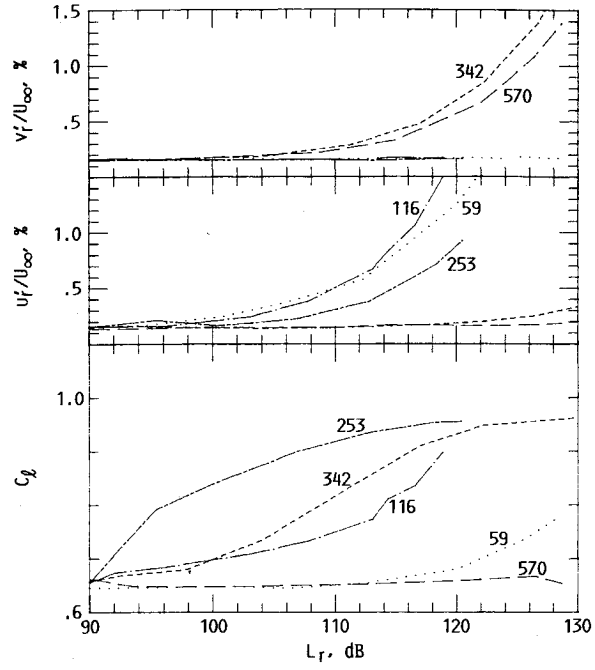

Fig. 7a Excitation amplitude effect on C_l at indicated f_p values. Reference u'_r and v'_r vs L_r shown on top. Same flow as that in Fig. 5.

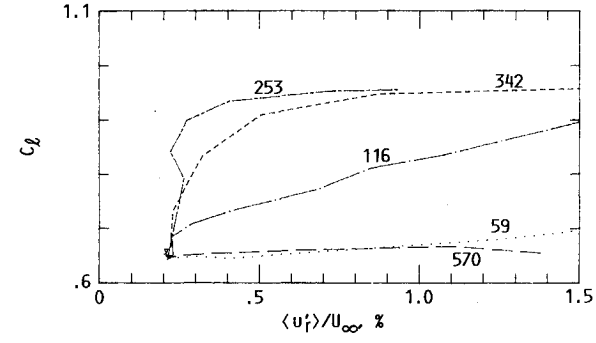

Fig. 7b C_l data of Fig. 7a cross plotted as a function of $\langle u'_r \rangle$.

that the induced v'_r and w'_r at these lower f_p are essentially the same as those without excitation. The amplitudes without excitation are represented by the left-hand-most data in the curves of Fig. 5; these amplitudes are somewhat overestimated due to noise from the anemometer circuitry.

The fundamental cross resonance due to the test section height occurs around 342 Hz. One finds that v'_r is very large at this frequency, but u'_r is practically zero. (Thus, a single hot wire at the reference location would fail to sense this resonance as v'_r is still only a small fraction of U.) Several peaks occur in the v'_r data, notably at 570, 995, 1400 Hz, etc. The frequencies of the cross resonances at a low Mach number are given by the following[14,15]:

$$f_{mn} = (a_0/2)\,[(m/H)^2 + (n/W)^2]^{1/2}$$

where m and n are integers, H and W are the height and width of the test section, respectively, and a_0 is the speed of sound.

Note that with the given orientation of the loudspeakers little w'_r fluctuation is induced. The woofer fails to excite the fundamental cross resonance in the z direction, which, if induced, should have marked the w'_r data by a peak around 224 Hz. Data similar to those in Fig. 5 were also obtained in the empty tunnel (airfoil removed) but with all other conditions remaining constant. Essentially similar amplitude variations were observed identifying the same major resonance peaks.

The u' and v' amplitudes were measured as a function of y (with the airfoil in) at $z = 0$ and $x = -11.4$ cm (Fig. 2) for a

few resonant frequencies. These are shown in Fig. 6a. Corresponding spanwise variations of the amplitudes are shown in Fig. 6b. These data indicate that the u' amplitude at 59 Hz is approximately constant over the entire cross section. Data at a few other low f_p (<280 Hz, not shown) also showed similar uniform amplitudes.

For $f_p = 342$ Hz and higher the v' data exhibit expected nodal patterns, which can also be used to identify the specific cross-resonance modes. Thus, the frequencies 342, 570, and 688 Hz can be identified as the f_{10}, f_{12}, and f_{20} modes, respectively. A frequency of 995 Hz appears to correspond to the f_{33} mode from the v' distribution, but the frequency computed from the equation of f_{mn} differs significantly. The difference remains unexplained; however, the tunnel conditions are not those of an idealized resonating duct, especially in view of the presence of the airfoil.

Choice of Excitation Amplitude

The excitation amplitude effect on various parameters is documented in Fig. 7a. For the flow under consideration the most pronounced effect on C_l occurs in the f_p range of 116–342 Hz. Inspection should reveal that, at 116 and 253 Hz, u'_r is large and v'_r is essentially zero, whereas the reverse is true for 342 Hz. Yet the flow is influenced at these frequencies in a consistent pattern. This indicates that inducing either perturbation velocity component upstream of the leading edge is equally effective in the excitation of the flow. This may not be surprising because, even when only v' fluctuation is induced upstream, it is converted, apparently via continuity, to u' fluctuation of comparable amplitude in the boundary layer over the airfoil (see Fig. 14 later).

In Figs. 5 and 6 it is generally observed that for a given f_p either u'_r is large and v'_r is small or vice versa. In the study of

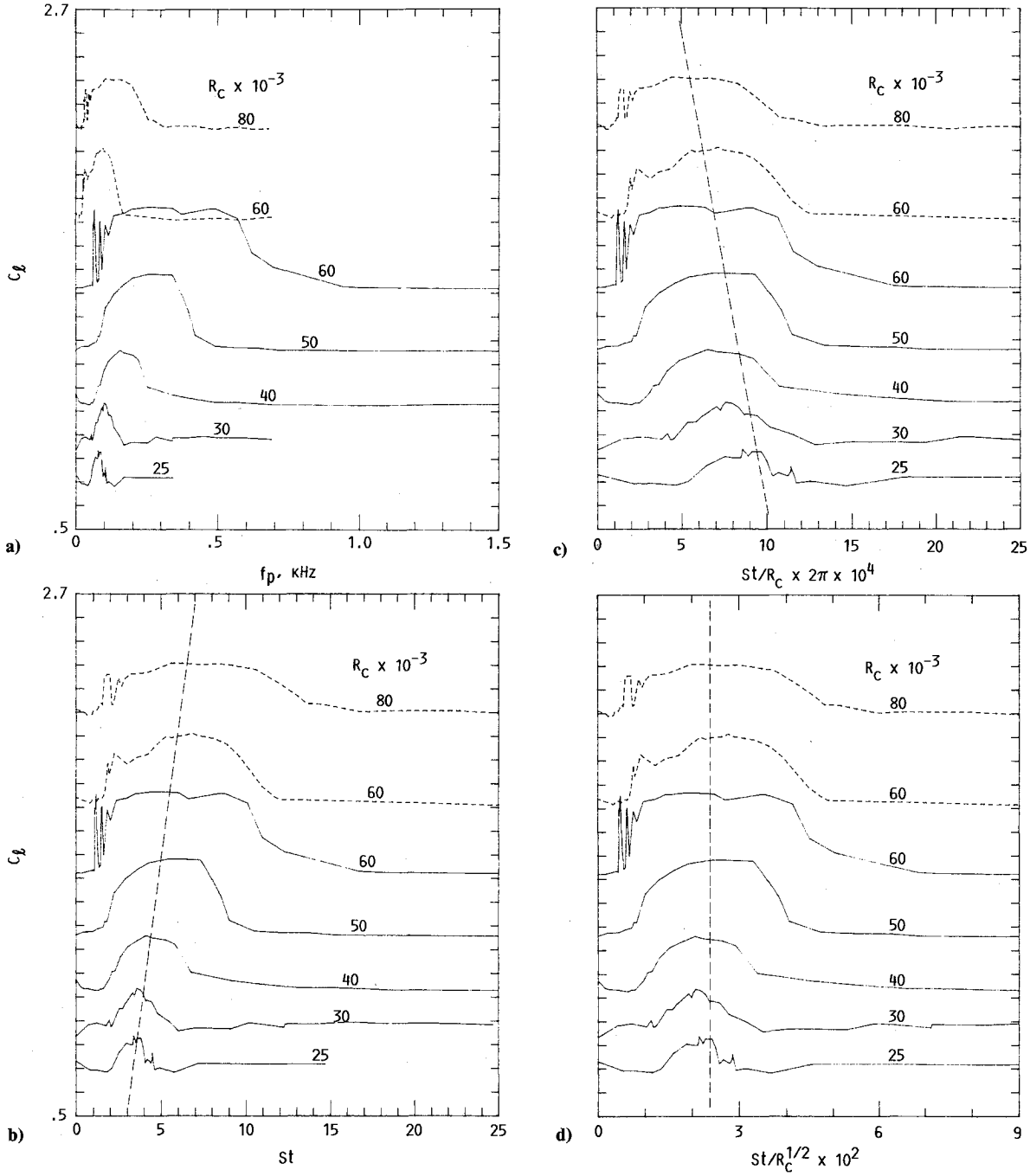

Fig. 8a C_l **vs for the LRN airfoils at** $\alpha = 6$ **deg;** $\langle u'_r \rangle / U_\infty = 0.005$**. Ordinate applies to bottom curve; others are staggered successively by two divisions. Solid lines,** $c = 12.7$ **cm model; dashed lines,** $c = 25.4$ **cm model. Figs. 8b–8d Data replotted as a function of indicated abscissas.**

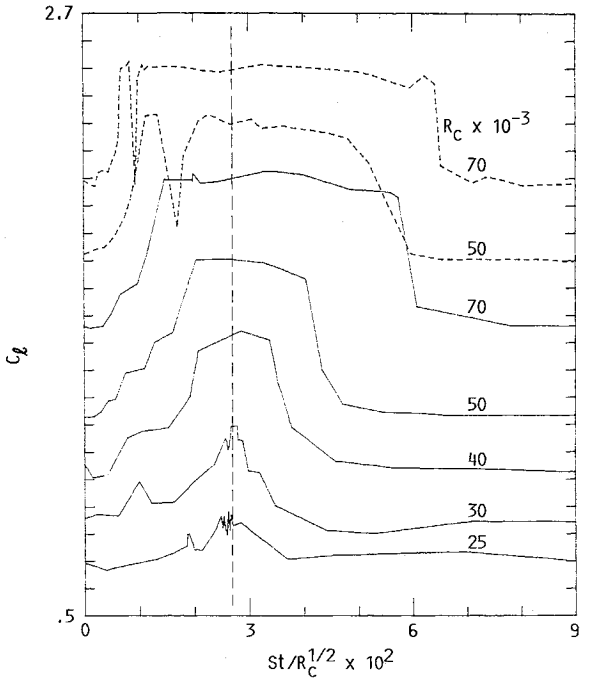

Fig. 9 Data, as in Fig. 8d, for the Wortmann airfoils.

excitation frequency effect it was desirable to keep a particular component of the perturbation velocity amplitude in the incoming flow a constant. However, because of the resonances it would be impossible to achieve that in a wind tunnel. Since inducing either u'_r or v'_r has a similar effect, it was decided that the resultant $\langle u'_r \rangle = (u'^2_r + v'^2_r)^{1/2}$ would be kept constant for the subsequent data. For the lower f_p (<280 Hz), this reasonably approximated the condition where u'_r was held constant in the incoming flow over the entire tunnel cross section. For specific modes such as f_{10} (= 342 Hz) and f_{30} (≈ 1026 Hz), this approximated a constant v'_r near the leading edge over the entire span of the airfoil. At other f_p the amplitude can be expected to be nonuniform. However, it should be obvious that $\langle u'_r \rangle$ at the chosen reference location should be a more meaningful amplitude parameter than a perturbation velocity amplitude elsewhere or the sound pressure level anywhere in the tunnel.[5,6] One could argue, from an instability point of view, that the u' amplitude near the separation point should have been a better reference. However, recall the complexities discussed in the Introduction; note that the separation point itself moves variably with varying excitation parameters. There is also the question of receptivity. In all likelihood the instability waves in the boundary layer are generated by the sound field near the airfoil leading edge. Therefore, the role of the boundary layer prior to separation cannot be completely ignored even though the amplification may be taking place primarily in the separated shear layer downstream. Thus, $\langle u'_r \rangle$ representing the perturbation level in the incoming flow was considered to be quite appropriate.

In Fig. 7b, C_l vs $\langle u'_r \rangle$ are cross plotted from the data of Fig. 7a. It is clear that around the "effective" frequency it takes a small amplitude to reattach the flow yielding the higher lift. The curves are seen to flatten out with increasing $\langle u'_r \rangle$, indicating that the flow has reattached optimally at the low amplitudes, leaving no room for further improvement. This made the measurement of the effective excitation frequency envelopes easier and relatively unambiguous. In other words, such an envelope measured for one value of $\langle u'_r \rangle$ should not be very different if a somewhat different value of $\langle u'_r \rangle$ were chosen. This also provided an assurance that the amplitude nonuniformities due to tunnel resonances may not have influenced these measurements critically. In the following, excitation only at a fixed, small amplitude is considered. A reference amplitude of $\langle u'_r \rangle / U_\infty = 0.5\%$ was chosen. At this amplitude, spectral analysis of u' and v' at the reference location for several f_p indicated "pure tone" excitation; higher harmonics were no larger than 2% of the fundamental in rms amplitude.

Effective Frequency Scaling

The excitation frequency effect is shown in Fig. 8a for the LRN airfoil. The data are shown from the lowest R_c where C_l could yet be resolved reliably with the given instrumentation to the highest R_c, above which the flow reattached naturally. There are data from airfoils of two different chords. Clearly, the effective f_p range increased and shifted to the right with increasing R_c for a given airfoil.

Figures 8b–8d are cross plots of the data of Fig. 8a as a function of the indicated abscissas. Inspection of these figures should convince one that the parameter $St/R_c^{1/2}$ best aligns the effective f_p bands. (The dashed straight lines are drawn to emphasize this point.) The same inference is made from the corresponding data for the Wortmann airfoil, for which the data are shown in Fig. 9 only in the format of Fig. 8d for space conservation. It is remarkable that a nondimensional parameter has emerged out of this exercise, at a given value of which, viz., at $St/R_c^{1/2} \approx 0.025$, the excitation is most effective for airfoils of two different cross sections, each with two different chords. Note that this relationship is equivalent to the most effective frequency scaling as $U_\infty^{3/2}$, the significance of which is discussed following the flowfield details.

Figure 10 shows additional data for the LRN airfoil at R_c = 50,000 for a few other angles of attack involving the laminar separation. The most effective excitation frequency again corresponds to $St/R_c^{1/2} \approx 0.025$ in all of the cases.

It is interesting to note here that preliminary flight experiments with a sailplane, conducted very recently by Peter C. Masak (private communication), indicated a significant drag reduction under excitation. For a 62-K-131 Wortmann wing section, 20% or more reduction in the profile drag was reported at $R_c \approx 10^6$. It is not clear if the phenomenology and the effect were the same as being studied here, however, the optimum f_p observed by Masak essentially followed the relationship stated above.

Flowfield Details

The flow at R_c = 50,000 for the c = 12.7 cm LRN airfoil at α = 6 deg was chosen for detailed measurements with and

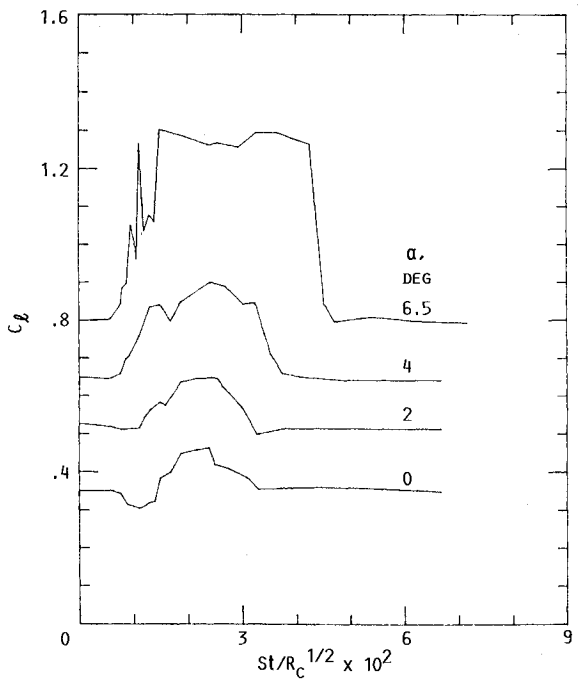

Fig. 10 Data as in Fig. 8d for the c = 12.7 cm LRN airfoil at R_c = 50,000 for four different α; $\langle u'_r \rangle / U_\infty$ = 0.005.

without excitation. The excitation was at 253 Hz corresponding to $St/R_c^{1/2} = 0.025$. Some of these data were obtained at an earlier time when the $\langle u'_r \rangle$ amplitude was not measured. It is estimated to be about 0.25% of U_∞ for these cases. However, C_l measured in conjunction with these data was high ($\approx$ 0.9), representing the plateau in the corresponding C_l curve of Fig. 7b. Thus, the difference in the amplitudes should not make a significant difference in the overall flowfields.

Figure 11 shows the distribution of $\langle U \rangle$ extrema around the airfoil, as explained in the following. These data were obtained by traversing a single hot wire (sensing the resultant of U and V, which is denoted $\langle U \rangle$). At a given x' on the upper surface, $\langle U \rangle$ was maximum near but outside the boundary layer and decreased slowly with increasing distance away from the airfoil surface. Underneath the airfoil the velocity outside the boundary layer was lower than U_∞ and slowly increased away from the airfoil. At $\alpha = 6$ deg, the rate of change of $\langle U \rangle$ with y outside the boundary layer was slow; thus, even if the hot wire was placed somewhat away, it reasonably measured the corresponding $\langle U \rangle$ extremum expected just outside the boundary layer. Thus, for measurement convenience the data of Fig. 11 were obtained by simply traversing the hot wire at a constant y each for the suction side and the pressure side. These data approximate the potential flow velocity distribution and can provide an estimate of the pressure coefficient (C_p) distribution. Note that the excitation enlarges the area within the $\langle U \rangle$ envelope, and hence within the C_p envelope, commensurate with the observed increase in lift. The quantity

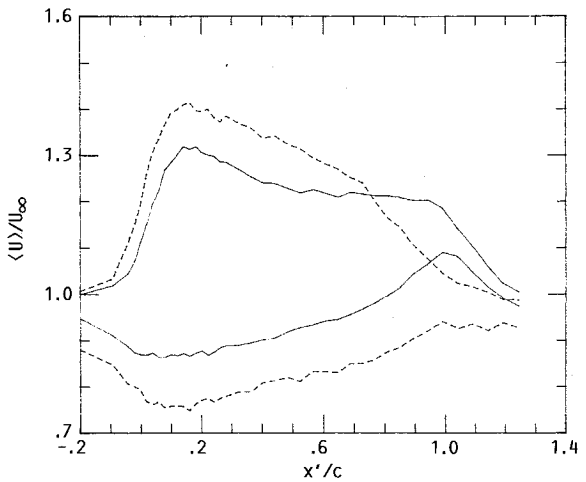

Fig. 11 $\langle U \rangle$ vs x' measured at constant y; $y = 1.65$ cm for the upper two curves; $y = -1.4$ cm for the lower two curves. Solid line, no excitation; dashed line, excitation at $f_p = 253$ Hz with $\langle u'_r \rangle / U_\infty = 0.005$. LRN airfoil at $\alpha = 6$ deg, $R_c = 50{,}000$.

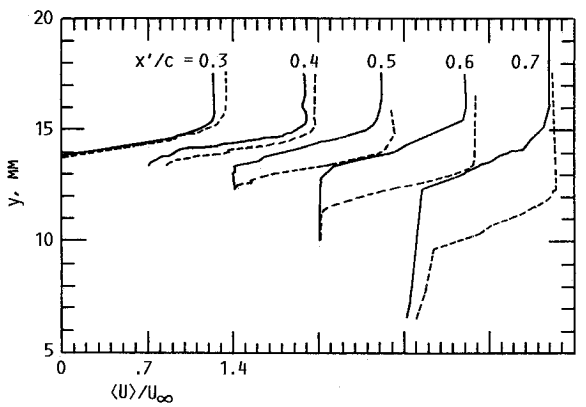

Fig. 12 Boundary-layer profiles of $\langle U \rangle$ at different x' for the same flow as that in Fig. 10. Solid lines, unexcited flow; dashed lines, excitation at $f_p = 253$ Hz and $\langle u'_r \rangle / U_\infty = 0.0025$. Abscissa applies to pair on left; others are shifted to the right successively by one major division.

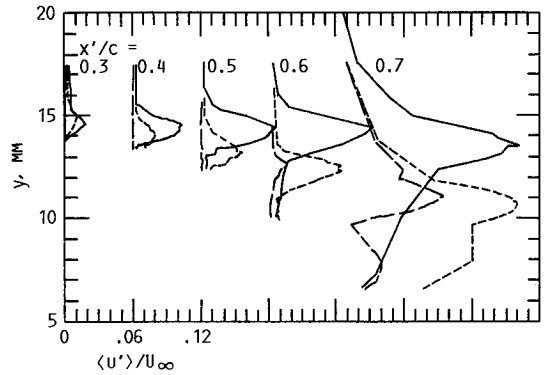

Fig. 13 Root-mean-square amplitude profiles corresponding to the data of Fig. 11. Solid line, total $\langle u' \rangle$ for the unexcited flow; short dashed line, total $\langle u' \rangle$ for the excited flow; long dashed line, fundamental $\langle uf \rangle$ for the excited flow. Successive set of curves shifted to right as in Fig. 11.

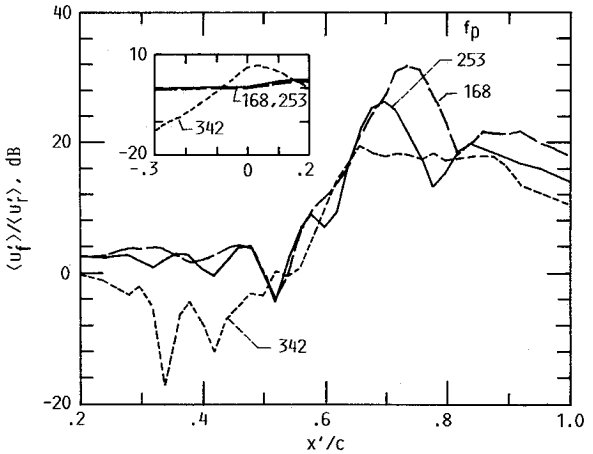

Fig. 14 $\langle uf \rangle$ vs x' measured along 70% velocity point on the upper surface for indicated f_p values. Same flow as that in Fig. 10; $\langle u'_r \rangle / U_\infty = 0.005$.

$(\delta\langle U \rangle / \delta x)(c/U_\infty)$ is found to be about -0.3 around the 30% chord location for both the excited and unexcited flows, with the same slope extending farther downstream for the excited case.

Figure 12 shows the boundary-layer mean velocity ($\langle U \rangle$) profiles at various streamwise locations on the upper surface of the airfoil. The curves are staggered laterally, but for each x' the pair of profiles with and without excitation are shown with the same scale. The lower end of each profile terminates on the airfoil surface. Near the surface the measurements involve errors due to hot-wire rectification during flow reversal in the separated flows. Nevertheless, the measured profiles are shown in their entirety as they provide an indication of the size of the separated regions. The flat segments in the profiles, prior to the increase in $\langle U \rangle$ with increasing y, should correspond to the separated regions. Clearly, the excitation reduces the size of the latter, and reattachment is achieved up to about 50% chord location. However, it is clear that complete reattachment has not occurred, and there exists a separated region even under the excitation, starting from approximately $0.5c$ downstream of the leading edge.

Estimates of the boundary-layer θ were obtained from these data. The integration was truncated at the point where $\langle U \rangle$ was 20% of local $\langle U \rangle$ maximum to avoid contribution from the erroneous data in the separated region. The integration was truncated on the other end at the 95% $\langle U \rangle$ maximum point. Note that this procedure results in θ being reasonably estimated in the upstream attached flows; however, it is underestimated in the separated region as the momentum defect in the reversed flow is not taken into account. However,

Table 1 Momentum thickness θ estimated from data of Fig. 12

x'/c	θ/c, Unexcited	θ/c, Excited
0.3	0.016	0.022
0.5	0.021	0.022
0.7	0.037	0.037

Table 2 Nondimensional frequency and wavelength estimated from data of Fig. 14

f_p, Hz	λ/c	$\lambda f_p/U_\infty$	$f_p\theta/U_\infty$
168	0.14	0.51	0.008
253	0.10	0.55	0.012
342	0.077	0.57	0.016

the magnitude of the reverse-flow velocity is small,[11] as also indicated by the profiles of Fig. 12. Thus, the error in θ due to the neglect of the reverse-flow momentum should be small.[11] Values of θ for three x locations are listed in Table 1. The Reynolds number and the Strouhal number of excitation, based on θ at $x'/c = 0.5$ for the excited flow, turn out to be 110 and 0.012, respectively.

The u' rms amplitude profiles in the boundary layer corresponding to the data of Fig. 12 are shown in Fig. 13. With the excitation the total fluctuation intensity is reduced somewhat at all stations. The fundamental amplitudes show that the instability wave, for the case documented, grows perceptibly beyond the 50% chord location, as will be discussed further. The fundamental amplitudes were measured by spectral analysis. The spectra traces have not been shown for space conservation.

The fundamental amplitude growth along the 70% velocity point was measured for three f_p and is shown in Fig. 14. The inset shows variations of the amplitudes upstream, not covered in the main figure, but along a constant height (y) passing through the 70% velocity point at $x'/c = 0.2$. The reference amplitude $\langle u'_r \rangle$ was held constant at 0.5% of U_∞. However, at 342 Hz only v' is induced upstream of the leading edge, with u' being very small (Fig. 5). Thus, the measured amplitude $\langle u'_f \rangle$ there is small since the single hot wire primarily senses the amplitude in the direction of the mean flow. As the leading edge of the airfoil is approached u' for 342 Hz becomes large, apparently via continuity of the perturbation field, as the presence of the wall restricts the v' fluctuation.

Downstream of the leading edge the amplitude variations show standing wave patterns, reminiscent of the acoustically excited boundary-layer data of Ref. 16. This occurs due to the interference of the excited instability wave and the exciting acoustic wave when the amplitudes of the two are comparable. The wavelength of the standing wave should exactly equal the shorter hydrodynamic (instability) wavelength (λ).[16] The value of λ for the three f_p was obtained from Fig. 14; λ and f_p provided the phase velocity of the instability wave. These quantities and the Strouhal number based on θ at $x'/c = 0.5$ are listed in Table 2.

One notes from Fig. 14 that the amplitudes rise sharply for all f_p past 50% chord location. Referring back to the boundary-layer profiles in Fig. 12, it is apparent that the amplification of the imposed disturbance takes place in the separated shear layer.

Further Comments on the Flowfield and its Stability

Let us consider further the observed frequency scaling, in Figs. 8–10, in light of the flowfield measurements. First, the measurements of the velocity gradient and the boundary-layer thicknesses are found to agree reasonably well with laminar separation criteria. Gaster[10] quoted Thwaite's laminar boundary-layer separation criterion as $\theta_s^2/\nu = -0.09/(\delta U/\delta x)$, where θ_s is the momentum thickness at incipient separation and $\delta U/\delta x$ the external velocity gradient (see also Ref. 17). Using this equation, the measured value of $\delta\langle U\rangle/\delta x = -0.3U_\infty/c$ yields a value of θ_s/c to be 0.024. This compares well with the value of 0.022 estimated from the boundary-layer measurements for the excited flow at $x'/c \approx 0.5$.

The extent of the separated region immediately downstream of the separation point also agrees with previous data on the divergence of the separating streamline. Using flow visualization, Dobbinga et al.[18] measured the angle (γ) between the separating streamline and the airfoil surface for a variety of laminar separation cases. The data fell nicely on a single curve given by $\tan(\gamma) = 15/(R_\theta)_{sep}$. The divergence of the separated region in Fig. 12 for the excited case yields a value of $\tan(\gamma)$ to be about 0.11, with corresponding R_θ being about 110. These values agree with the aforementioned equation.

The question that then naturally arises is whether the criterion $St/R_c^{1/2} \approx 0.025$ for the most effective f_p could be expected from stability considerations. A satisfactory analysis of the stability of a separating boundary layer, including the aspects discussed in the Introduction, is unavailable at this time. The value of $f_p\theta_s/U_\infty \approx 0.012$ corresponding to the most effective f_p for $R_c = 50{,}000$ is found to agree reasonably with inviscid stability analysis for a separated boundary layer. Van Ingen[19] carried out such an analysis for the Falkner-Skan flows. For the separated-flow case he found the maximally unstable frequencies to correspond to $f_p\theta/U_\infty \approx 0.01$ for a range of the pressure gradient parameter, in reasonable agreement with the data previously given. It is not clear whether the relationship $f_p\theta/U_\infty \approx 0.01$ will hold under a wider combination of parametric ranges and whether an inviscid analysis will be sufficient to explain the presently observed relationship of $St/R_c^{1/2} \approx 0.025$. Needless to say, more work, including experiments, will be required to completely understand the mechanisms involved in this class of flows.

Conclusion

Small-amplitude acoustic excitation at an appropriate frequency can effectively reduce laminar separation occurring on the suction side of airfoils at low α and low R_c. This results in a significant improvement in the lift coefficient. It is inferred from data with airfoils of two cross-sectional shapes, each with two different chords, that the optimum effect occurs when the parameter $St/R_c^{1/2}$, corresponding to the excitation frequency, falls in the range of 0.02–0.03. Detailed flowfield data recorded for a specific case indicate that a separated region still exists under the excitation, and the amplification of the imposed perturbation takes place primarily in the downstream shear layer rather than in the upstream boundary layer.

References

[1]Collins, F. G., and Zelenevitz, J., "Influence of Sound upon Separated Flow Over Wings," *AIAA Journal,* Vol. 13, No. 3, 1975, pp. 408–410.

[2]Carmichael, B. H., "Low Reynolds Number Airfoil Survey: Vol. I," NASA Contractor Rept. 165803, 1981.

[3]Mueller, T. J., and Batill, S. M., "Experimental Studies of Separation on a Two-Dimensional Airfoil at Low Reynolds Numbers," *AIAA Journal,* Vol. 20, No. 4, 1982, pp. 457–463.

[4]Ahuja, K. K., and Burrin, R. H., "Control of Flow Separation by Sound," AIAA Paper 84-2298, 1984.

[5]Zaman, K. B. M. Q., Bar-Sever, A., and Mangalam, S. M., "Effect of Acoustic Excitation on the Flow Over a Low-*Re* Airfoil," *Journal of Fluid Mechanics,* Vol. 182, 1987, pp. 127–148.

[6]Neuburger, D., and Wygnanski, I., "The Use of a Vibrating Ribbon to Delay Separation on Two-Dimensional Airfoils: Some Preliminary Observations," Workshop on Unsteady Separated Flow, Air Force Academy, July 1987 (Private Communication).

[7]Huang, L. S., Maestrello, L., and Bryant, T. D., "Separation Control Over An Airfoil at High Angles of Attack by Sound Emanating from the Surface," AIAA Paper 87-1261, 1987.

[8]Hsiao, F., Liu, C., Shyu, J., and Wang, M., "Control of Wall-Separated Flow By Internal Acoustic Excitation," AIAA Paper 89-0974, 1989.

[9]Zaman, K. B. M. Q., McKinzie, D. J., and Rumsey, C. L., "A Natural Low Frequency Oscillation of the Flow Over An Airfoil Near Stalling Conditions," *Journal of Fluid Mechanics,* Vol. 202, 1989, pp.

403–442.

[10]Gaster, M., "The Structure and Behaviour of Laminar Separation Bubbles," AGARD CP-4, 1966, pp. 813–854.

[11]Schmidt, G. S., and Mueller, T. J., "Analysis of Low Reynolds Number Separation Bubbles Using Semiempirical Methods," *AIAA Journal,* Vol. 24, No. 8, 1989, pp. 993–1001.

[12]Nishioka, M., Asai, S., and Yoshida, S., "Control of Flow Separation by Acoustic Excitation," AIAA Paper 89-0973, March 1989.

[13]Goldstein, M. E., "Generation of Instability Waves in Flows Separating from Smooth Surfaces," *Journal of Fluid Mechanics,* Vol. 145, 1984, pp. 71–94.

[14]Goldstein, M. E., *Aeroacoustics,* McGraw-Hill, New York, 1976.

[15]Baumeister, K. J., "Reverberation Effects on Directionality and Response of Stationary Monopole and Dipole Sources in a Wind Tunnel," *Journal of Vibration, Stress and Reliability in Design,* Vol. 108, 1986, pp. 82–90.

[16]Leehey, P., and Shapiro, P., "Leading Edge Effect in Laminar Boundary Layer Excitation by Sound," *Proceedings of the IUTAM Symposium on Laminar Turbulent Transition,* Springer-Verlag, Berlin, 1977, pp. 321–331.

[17]Schlichting, H., *Boundary Layer Theory,* McGraw-Hill, New York, 1979.

[18]Dobbinga, E., Van Ingen, J. L., and Kooi, J. W., "Some Research On Two-Dimensional Laminar Separation Bubbles," AGARD CP-102, 1972.

[19]Van Ingen, J. L., "On The Calculation Of Laminar Separation Bubbles in Two-Dimensional Incompressible Flow," AGARD CP-168, 1975, pp. 11.1–11.16.